JOURNAL OF PROPULSION AND POWER
Vol. 22, No. 5, September–October 2006

Forced Response of a Swirling, Premixed Flame to Flow Disturbances

Benjamin D. Bellows,* Yedidia Neumeier,† and Timothy Lieuwen‡
Georgia Institute of Technology, Atlanta, Georgia 30324

This paper presents measurements of the nonlinear response of a premixed flame to harmonic oscillations. These measurements were obtained to improve understanding of nonlinear flame dynamics in unstable combustors. Simultaneous measurements of CH* and OH* chemiluminescence, pressure, and velocity were obtained over a range of forcing amplitudes and frequencies. These data show that the flame chemiluminescence response to imposed oscillations saturates at pressure and velocity amplitudes on the order of $p'/p_0 \sim 0.02$ and $u'/u_0 \sim 0.3$. The value of the fluctuating to the mean chemiluminescence signal at saturation varied with equivalence ratio. The phase between the chemiluminescence and acoustic signal also exhibits substantial amplitude dependence, even at driving levels where their amplitude ratios are nearly linear. In contrast, the pressure-velocity relationship remains linear with constant phase over the entire amplitude range. Thus, these results suggest that the nonlinear dynamics of premixed combustors are controlled by the acoustics-heat-release relationship, as opposed to gas dynamical processes. The mechanism for saturation of the flame response appears to be caused by nonlinear interactions between the flow forcing and the parametric flame instability, possibly through their impact on the fluctuating flame position. This parametric instability occurs at half the forcing frequency and is caused by the oscillating flow acceleration in the presence of the density jump at the flame. To our knowledge, this observation of the parametric instability is the first in a turbulent, swirl-stabilized flame. Interactions between the nonlinear heat release and linear combustor acoustics were characterized by sweeping the driving frequency through a resonant combustor frequency. With increasing driving amplitude, the resulting frequency response curves began to saturate in amplitude and bend over toward lower frequencies. Similar to the classical nonlinear Duffing oscillator, this bending of the frequency response curves manifests itself as a subcritical bifurcation in combustor response, whose gain and phase exhibited jumps and hysteresis. The bifurcation structure was measured in detail over a range of conditions and shown to have a two-dimensional dependence upon both amplitude and frequency.

Nomenclature

f	=	frequency
p	=	pressure
Q	=	heat release
t	=	time
u	=	velocity
γ_{ij}	=	coherence between quantities i and j
Δ	=	uncertainty estimate in measurements
θ_{ij}	=	phase angle between quantities i and j
ϕ	=	equivalence ratio
ω	=	angular frequency, $=2\pi f$

Subscript and Superscript

0	=	mean quantity
$'$	=	fluctuating amplitude

I. Introduction

THIS paper describes an experimental investigation of the relationship between flow disturbances and heat-release oscillations in a lean, premixed combustor. This work is motivated by the fact that combustion instabilities continue to be one of the most serious issues hindering the development and operation of industrial gas turbines.[1–5] These instabilities generally occur when the unsteady combustion process couples with one or more of the natural acoustic modes of the combustion chamber, resulting in self-excited oscillations. These oscillations adversely affect engine performance and emissions and can be destructive to engine hardware.

Our focus here is on the amplitude response of the heat release at some frequency f to a harmonic disturbance of amplitude A at that same frequency. The heat-release response $H(A)$ generally exhibits a linear dependence upon the disturbance amplitude at small values of A. At high amplitudes, however, they are related nonlinearly. This is significant because the dynamics of an unstable combustor are controlled by both linear and nonlinear processes. This can be seen from Fig. 1, which plots the amplitude dependence of hypothetical driving $H(A)$ and damping $D(A)$ processes. Note that the disturbance amplitude stays the same, decreases, or increases depending upon whether $H(A) = D(A)$, $H(A) < D(A)$, or $H(A) > D(A)$, respectively. Linear combustor processes generally control the balance between driving and damping processes at low amplitudes of oscillation and, thus, determine the frequency and growth rate $A \sim e^{\alpha t}$ of inherent disturbances in the combustor. Note that the initial growth rate of the instability α is proportional to the difference between the driving and damping processes in the linear regime $H(A) - D(A)$. Nonlinear combustor processes control the finite-amplitude dynamics of the oscillations. For example, predicting the limit-cycle amplitude of self-excited oscillations requires an understanding of the nonlinear characteristics of $H(A)$ and $D(A)$. To illustrate, Fig. 1 depicts a situation where $H(A)$ saturates and $D(A)$ remains linear, so that the two curves cross at the limit-cycle amplitude A_{LC}.

Understanding of a combustor's linear dynamics is needed to predict the frequency and conditions under which inherent disturbances in the combustor grow or decay. As a result of extensive work in this area, capabilities for modeling the acoustics of the combustor

Presented as Paper 2004-0455 at the AIAA 42nd Aerospace Sciences Meeting, Reno, NV, 5–9 January 2004; received 29 April 2005; accepted for publication 11 December 2005.

*Graduate Research Assistant, School of Aerospace Engineering, Aerospace Combustion Lab, 635 Strong Street, NW; currently Research Engineer, Pratt & Whitney, 400 Main Street, East Hartford, CT 06108; benjamin_bellows@aerospace.gatech.edu. Member AIAA.

†Senior Research Engineer, School of Aerospace Engineering, 270 Ferst Drive, NW. Member AIAA.

‡Associate Professor, School of Aerospace Engineering, 270 Ferst Drive, NW. Senior Member AIAA.

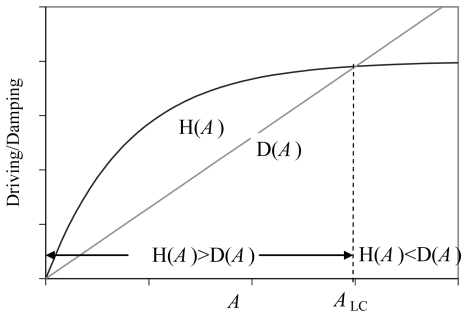

Fig. 1 Qualitative description of the dependence of acoustic driving $H(A)$ and damping $D(A)$ processes upon amplitude of oscillation A.

system are reasonably well developed (e.g., see Refs. 6 and 7). Also, capabilities for modeling the interactions of flow and mixture disturbances with flames, needed to predict the conditions under which instabilities occur, are improving rapidly.[8,9] Much of this work is being transitioned to industry and being incorporated into dynamics predictions codes. In fact, most gas-turbine manufacturers have reported model development efforts for predicting instability frequencies, mode shapes, and conditions of occurrence.[10–12]

As just noted, understanding of a combustor's linear dynamics is not sufficient to describe the finite-amplitude dynamics of self-excited oscillations, for example, for predicting the limit-cycle amplitude. The need to predict instability amplitudes and observations of "triggered" instabilities in rockets that were linearly stable motivated past workers to consider these nonlinear effects, for example, see Refs. 6 and 13–15. Much of this work focuses on the role of nonlinear gas dynamics in combustors, however. As such, it is likely more relevant to instabilities in combustion systems where fluctuating pressure amplitudes achieve significant percentages of the mean (e.g., $p'/p_0 \sim 20$–50%, such as is observed in rockets), than lean premixed gas-turbine combustors where reported instability pressure amplitudes are typically on the order of 1–5% of the mean pressure.[2,16]

Recent studies[16–19] suggest that acoustic processes essentially remain in the linear regime, even under limit-cycle operation, and that it is the nonlinear relationship between flow and heat-release oscillations which causes saturation of the instability amplitude. As such, the flame's nonlinear response to harmonic disturbances can play a critical role in the overall dynamics of an unstable combustor. For example, Dowling[17] introduced a phenomenological model for the finite-amplitude response of a flame to velocity perturbations. The model is dynamic in nature, but the essential nonlinearity consists of a quasi-steady relation between flow velocity and heat-release rate. It assumes a linear relation between the heat release Q and velocity perturbation when the total velocity $[u(t) = u_0 + u'(t)]$ lies between 0 and $2u_0$. When $u(t) < 0$, the heat release goes to zero, and when it is greater than $2u_0$ it saturates at $2Q_0$. Thus, the essential mechanism of nonlinearity lies in the fact that the lowest amplitude of heat-release oscillation cannot indefinitely decrease with perturbation amplitude because it cannot achieve negative values. A similar mechanism was proposed in an experimental study of Poinsot et al.[20] In another study, Dowling[21] introduced a nonlinear boundary condition at the flame anchoring point. She assumed that the instantaneous flame anchoring point was fixed when the total gas velocity exceeded the flame speed. When the gas velocity fell below the flame speed, the former condition was replaced by one that allowed the flame to propagate upstream. Peracchio and Proscia[18] developed a quasi-steady nonlinear model to describe the response of the flame-to-equivalence-ratio perturbations. They assumed the following relationship for the response of the instantaneous mixture composition leaving the nozzle-exit-to-velocity perturbations:

$$\phi(t) = \bar{\phi}/[1 + ku'(t)/\bar{u}] \tag{1}$$

where k is a constant with a value near unity. They also utilized a nonlinear relationship relating the heat release per unit mass of mixture to the instantaneous equivalence ratio. Wu et al.[19] developed a more general asymptotic analysis that focuses on the nonlinear interaction/coupling among acoustic, vortical, and Darrieus–Landau instability modes at the flame. This theory is found to agree well with the experimental work presented in Searby.[22]

Several of the preceding analyses suggest that the ratio of fluctuating and mean velocity u'/u_0 is an important nondimensional parameter that controls the amplitude of the limit-cycle oscillations through its effect upon the nonlinear relationship between flow disturbances and heat-release oscillations. A similar conclusion was reached empirically in an experimental study of Lieuwen,[16] who found that combustion instability amplitudes had a strong dependence upon a mean combustor velocity scale u_0.

In an effort to understand the mechanisms controlling the growth rates and limit-cycle amplitudes of combustion instabilities, the response of the flame under external forcing of the flowfield has been analyzed by several researchers (e.g., see Refs. 23–27). Külsheimer and Büchner[23] measured the effect of driving frequency and amplitude on premixed swirled and unswirled flames. They characterized the conditions under which large-scale coherent ring-vortex structures were evident, a key mechanism for self-excited oscillations, as well as the resulting flame response, on driving amplitude and frequency. They found that vortex formation occurred at lower driving amplitudes as the driving frequency was increased. Furthermore, the peak flame response in swirl flames shifted to higher frequencies for larger flow perturbations. No explicit characterization of the nonlinear interaction between the flame's heat release and the flow perturbations was reported, however.

The potentially significant nonlinear relationship between acoustic perturbations and heat-release perturbations suggested by the preceding theoretical studies is also supported by recent measurements of Lieuwen and Neumeier,[24] Lee and Santavicca,[25] and Balachandran et al.,[27] who characterized the pressure-heat-release relationship as a function of oscillation amplitude. The former study found that this relationship was linear for pressure amplitudes below about 1% of the mean pressure. At higher forcing levels, they found that the heat-release oscillation amplitude began to saturate. In contrast to the assumed model of Dowling,[17] however, Lieuwen and Neumeier found saturation to occur at $CH^{*'}/CH^{*}_0$ values of $\sim$25%, in contrast to the 100% value assumed in her model. Data were only obtained at one operating condition and two driving frequencies; however, so the manner in which these saturation characteristics depend upon operating conditions and frequency is unclear.

Durox et al.[28] and Bourehla and Baillot[26] appear to have performed the only systematic study characterizing the response of a nonswirling flame to large-amplitude perturbations. Their study was performed on a laminar Bunsen flame and primarily focused on its qualitative characteristics. No measurements of the dependence of unsteady heat release or chemiluminescence emissions were reported. They found that at low frequencies ($f < 200$ Hz) and velocity amplitudes ($u'/u_0 < 0.3$) the flame front wrinkles symmetrically about the burner axis because of a convected wave traveling from the burner base to its tip. With increasing amplitude of low-frequency velocity perturbations, they found that the flame exhibited a variety of transient flame-holding behavior, such as flashback, asymmetric blowoff, and unsteady lifting and reanchoring of the flame. In addition, they noted that its response was asymmetric and disordered. Finally, at high frequencies and forcing amplitudes ($u'/u_0 > 1$), they found that the flame tip collapses to a hemispherical shape.

As can be seen from the preceding review, there is a need for systematic measurements of the flame's nonlinear response to flow perturbations, that is, saturation of the curve $H(A)$ in Fig. 1. Such characteristics must be understood in order to, for example, predict instability amplitudes or model the transient response of a combustor to active control. As such, we obtained measurements of the pressure/velocity/chemiluminescence amplitude and phase relationships in a swirling flame over a range of driving amplitudes. These results were obtained by externally driving oscillations in the combustor with varying amplitudes. Measurements were obtained at several driving frequencies and fuel/air ratios.

II. Experimental Facility and Instrumentation

A. Gas-Turbine Combustor Simulator

The data presented in this paper were measured in a lean, premixed gas-turbine combustor simulator, shown in Fig. 2, which has been previously described in Lieuwen et al.[29] Tests were performed at a mean pressure of 1.7 atm and mean equivalence ratios ranging from 0.83 to 1.0. All tests were performed at a total flow rate of 5.5 g/s, which corresponds to a premixer velocity of 11.5 m/s. Inlet temperatures were kept constant at room temperature.

The facility consists of inlet, combustor, and exhaust sections. High-pressure natural gas and air are supplied from building facilities, whose flow rates are measured with calibrated critical orifices. To ensure that acoustic oscillations do not affect fuel/air mixing processes, the air and fuel are introduced upstream of a second choke point, well upstream of the swirler. Thus, the equivalence ratio of the reactive mixture entering the flame is essentially constant. This was done because of the sensitivity of the flame chemiluminescence levels to both heat-release rate and equivalence ratio. If the equivalence ratio and heat-release rate simultaneously vary, monitoring the flame chemiluminescence alone would not be sufficient to infer information about heat-release fluctuations.[25] Note that the fuel/air mixing processes were not acoustically isolated in the previous study of Lieuwen and Neumeier.[24]

The fuel-air mixture enters the circular 4.75-cm-diam, 60-cm-long inlet section and passes through a 45-deg swirler prior to entering the combustor (see Fig. 3). Combustion occurs in the $5 \times 5 \times 51$ cm square combustor downstream of the conical flame holder, and the combustion products then flow through a circular 7.6-cm-diam, 195-cm-long exhaust section before leaving the system. A separate high-pressure airstream cools the combustor walls and mixes with the combustion products in the exhaust section. The flow leaves the setup through an exhaust nozzle.

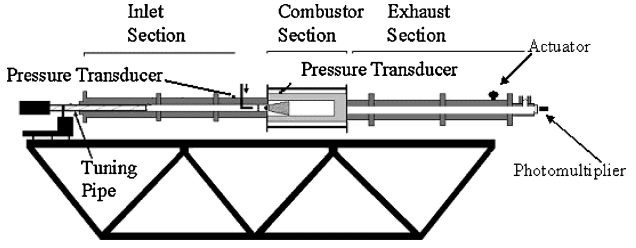

Fig. 2 Schematic of Georgia Tech lean, premixed combustor facility.

B. Instrumentation

Pressure oscillations were measured with two Model 211B5 Kistler pressure transducers mounted in the inlet section and combustor. These transducers are mounted 33.2 cm upstream and 5.1 cm downstream of the conical flame holder, respectively. The latter transducer was flush mounted and water cooled. The instantaneous velocity was measured with a hot-film probe mounted 23 cm upstream of the swirler and oriented perpendicular to the inlet flow in the radial center of the inlet pipe, as shown in Fig. 3. The fluctuating velocity at the premixer exit, used to define the flame transfer function, was determined by measuring the transfer function between the velocity oscillations at the hot-wire location and the premixer exit in off-line experiments. This transfer function was also calculated with a quasi-one-dimensional analysis by discretizing the premixer domain into a series of regions characterized by their lengths and cross-sectional areas and applying momentum and energy conservation at the interfaces (see Ref. 7). The swirler was modeled as a resistance that was determined from the flow velocity and measured mean pressure drop. The model and measurements agreed very well over the 10–550-Hz frequency range, except in transfer function magnitude in the vicinity of 80 and 420 Hz. At these frequencies, the transfer function has large values (on the order of 5) and the model and measurements disagree by 100% in the peak magnitude; however, they agree quite well in predicting the frequencies at which these occur. At all other frequencies, the transfer function magnitude is essentially constant and equal to the cross-sectional area ratio between the two points, as expected from quasi-steady considerations. Because of the sensitive frequency dependence of the velocity transfer function between the measurement location and premixer exit plane at 80 and 420 Hz, no forced response studies were performed at these frequencies.

Global CH^* and OH^* chemiluminescence measurements were obtained with a photomultiplier tube (PMT) fitted with 10-nm bandwidth filters centered at 430 and 310 nm, respectively. The PMT was installed downstream of a quartz window at the rear end of the setup (see Fig. 2). This arrangement permitted it to view the entire combustion zone. The linearity of the PMT output was verified over the entire range of instantaneous light intensity levels seen in these experiments. Data were obtained with a National Instruments DAQ controlled by Labview software at a sampling rate of 10 kHz. A total of 16,384 data points were taken during each test.

Oscillations were driven in the combustor with an actuator developed at Georgia Tech for active combustion control applications.[30] The actuator was mounted 5 m downstream of the flame zone. The actuator modulates a constant secondary supply of air that

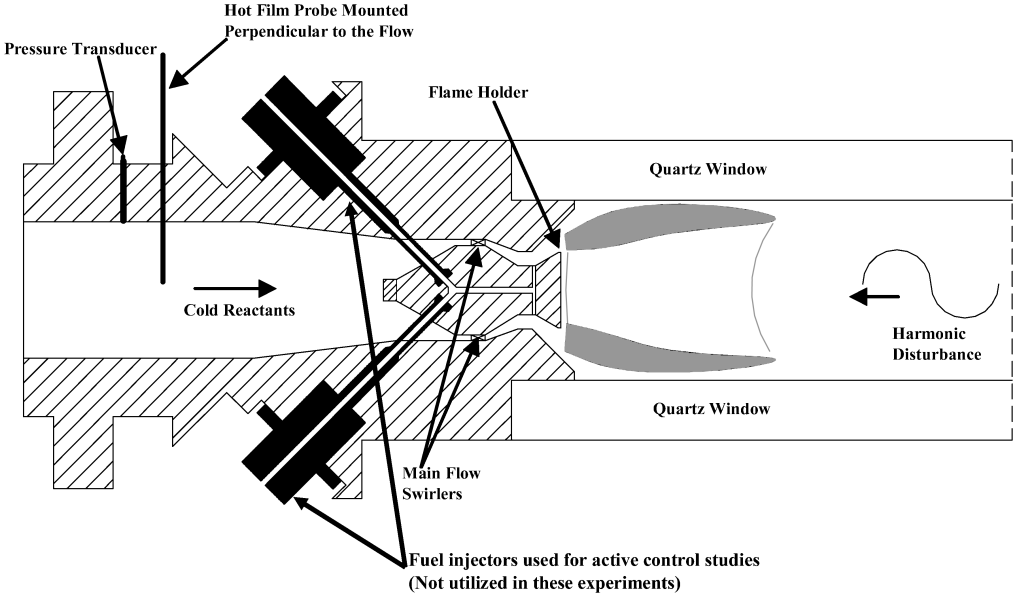

Fig. 3 Detail of mixing and combustion section.

is introduced near the combustor exit by periodically varying the degree of constriction of a valve. Maximum amplitude of driving occurs when the flow passage is completely blocked for a portion of the cycle, and, thus, the actuator modulates 100% of the flow through the valve. The amplitude of forcing can be controlled via the supply pressure of air to the actuator.

III. Forced Flame Characteristics

The basic experimental procedure consists of externally driving oscillations in the combustor with varying amplitude at a fixed frequency or fixed amplitude at varying frequencies while obtaining simultaneous measurements of pressure, velocity, and chemiluminescence. For all cases, the combustor was quite stable in the absence of driving. The flame length ranged from 5–15 cm between the equivalence ratios of 1.0–0.83, respectively.

A. Driving Effects on Average Flame and Coherence Characteristics

In addition to exciting oscillations, the imposed driving altered the mean flame characteristics, similar to prior observations (e.g., see Ref. 31). With increased driving levels, the flame's time-averaged length increased by up to 100%. In addition, its global intensity generally decreased very slightly, but not always in a monotonic manner. Typical results are shown in Fig. 4. In general, OH^* and CH^* levels were found to exhibit similar dependence upon disturbance amplitude.

To obtain accurate transfer function data, it is important to have good coherence between the pressure, velocity, and chemiluminescence oscillations at the frequency of interest. This was always achieved except at the lowest driving amplitudes; typical coherence values were greater than 0.95. The effect of nonlinearities is to also decrease the coherence value, and so we would not expect perfect coherence values, even if the input-output variables were perfectly correlated.

The amplitudes of the oscillations were determined by integrating the area under the power spectrum in the vicinity of the driving frequency. The rms levels of the oscillations were determined from these values via Parseval's relation and then multiplied by $\sqrt{2}$ to obtain the fluctuating amplitude. This procedure is equivalent to determining the fluctuating amplitude after bandpass filtering the signal about the driving frequency. The phases of the fluctuating parameters were determined from their Fourier transforms at the driving frequency.

B. Linear Flame Response

Baseline measurements of the linear flame response were obtained by driving oscillations at low amplitudes over the 10–550-Hz frequency range. The amplitude of the velocity-CH^* transfer function is plotted in Fig. 5a. The uncertainties were determined using formulas from Ref. 32.

This transfer function apparently has local maxima at 90 and 240 Hz and monotonically decays in the 250–400-Hz region. Similar peaks at intermediate frequencies were reported experimentally by Külsheimer and Büchner.[23] The corresponding phase of the transfer function is plotted in Fig. 5b. The phase results exhibit a linear increase with frequency up to approximately 400 Hz. This phase dependence suggests a roughly constant time delay relationship between the pressure/velocity and chemiluminescence, i.e., $CH^*(t) \sim u'(t-\tau)$. This time delay can be estimated from the slope of this phase dependence to yield a value of approximately 3.5 ms. For reference, the time required for a disturbance to convect the length of the approximately 8-cm flame at the premixer exit velocity is $\tau_{\text{flame}} \sim 7$ ms. This linear phase dependence ceases at frequencies above 400 Hz as the phase dips then rises again. Recall, however, that the transfer function between the velocity oscillations at the measurement point and flame base changes rapidly in the vicinity of 80 and 420 Hz. Thus the results at these frequencies should be interpreted with caution.

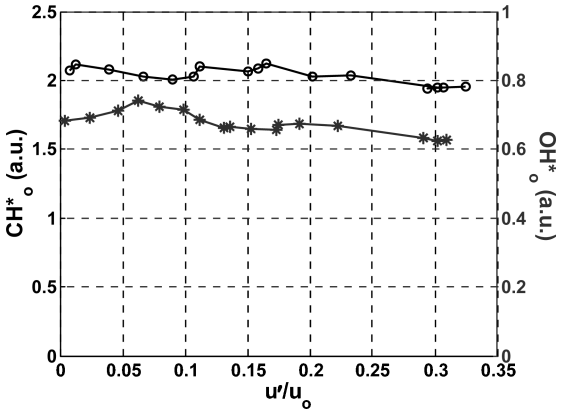

Fig. 4 Dependence of mean CH^* and OH^* signals upon velocity oscillation amplitude ($f_{\text{drive}} = 280$ Hz, $\phi = 0.95$).

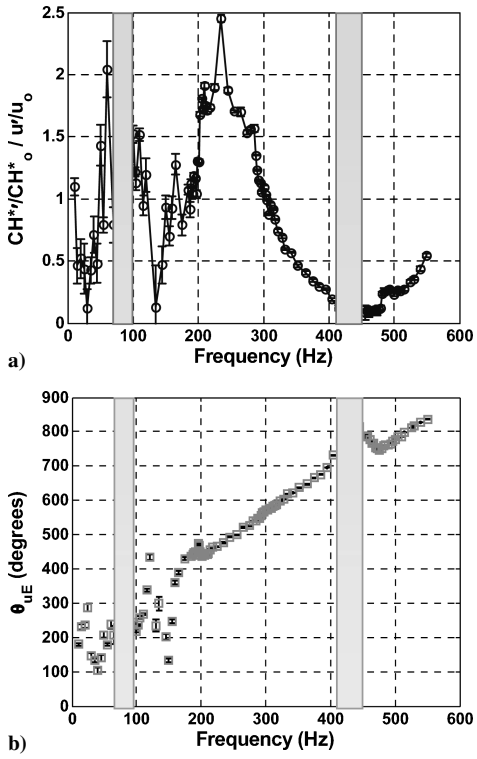

Fig. 5 Dependence of a) linear velocity-CH^* transfer function and b) velocity-CH^* phase angle upon driving frequency.

It is interesting to note the similarities between these gain and phase results and the measured and predicted transfer functions reported by Schuller et al.[23] This is interesting because they obtained their results for a laminar flame while our data are obtained from a swirling, turbulent flame. Apparently, the average V shapes of the two flames are the primary thing they have in common. This observation indicates that the theoretical result used to describe laminar flame dynamics can be fit to our data very satisfactorily.

IV. Nonlinear Flame Response

Next, we consider the amplitude dependence of this transfer function. For brevity, only velocity results are presented because the pressure-velocity relationship is linear over the entire driving amplitude range, for example, see Fig. 6. Therefore, the p'-CH^* transfer function has an identical form (although the results are "cleaner" because of the larger p'-CH^* coherence values). Figure 7a presents typical results showing the dependence of the normalized CH^* and OH^* chemiluminescence amplitudes upon the normalized velocity amplitudes over a range of driving amplitudes. The departure of this transfer function from linearity is illustrated by comparing the data with the solid line that is drawn in. (The reason for the gap in the data is discussed in the "Nonlinear Heat Release-Linear Acoustics Interaction" section.) Note also in Figs. 6 and 7 that the normalized

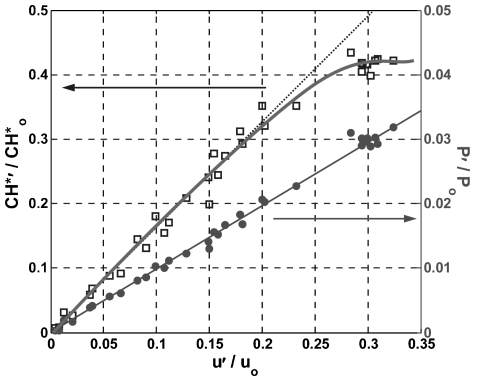

Fig. 6 Dependence of CH* chemiluminescence and pressure oscillation amplitude on velocity fluctuation amplitude ($f_{drive} = 280$ Hz, $\phi = 0.95$).

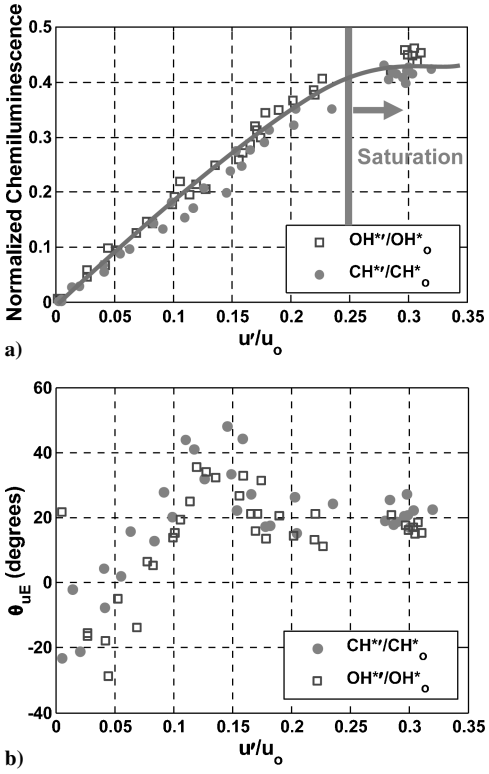

Fig. 7 Dependence of CH* and OH* chemiluminescence a) amplitude and b) phase angle on velocity oscillation amplitude. Chemiluminescence saturation occurs in a) at $u'/u_0 > 0.25$, Uncertainty in phase angle for $u'/u_0 < 0.05$, $\Delta\theta \sim 30$ deg; for $u'/u_0 > 0.05$, $\Delta\theta \sim 2$ deg ($f_{drive} = 283$ Hz).

amplitudes of the pressure and velocity oscillations at the point where nonlinear effects become abvious are roughly 3 and 30% while the normalized chemiluminescence is approximately 40%. These relatively low-pressure fluctuations and significant chemiluminescence oscillations are consistent with speculations that heat-release nonlinearities, as opposed to gas dynamic ones, control the nonlinear dynamics of premixed combustion systems. These pressure amplitudes where nonlinearities in the p'-CH* relationship are observed ($p'/p_0 \sim 2$–3%) are of similar magnitude as typical instability amplitudes ($p'/p_0 \sim 0.5$–2%), which were measured in other tests on this combustor.[29] Also, the amplitude of the normalized CH* oscillations is on the order of 30–40% of the mean, consistent with previous experiments.[24]

Figure 7b presents the phase relationship between the velocity oscillations and the normalized chemiluminescence. The figures indicate that the phase angle has a complex dependence on the amplitude of oscillations. It increases monotonically by about

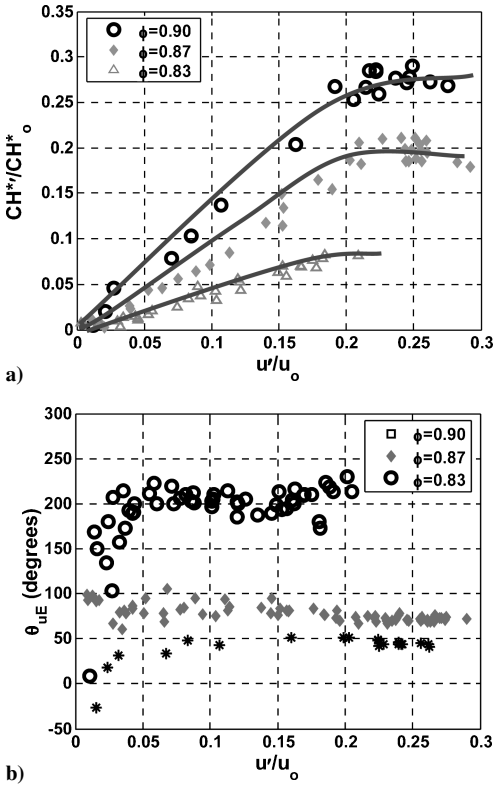

Fig. 8 Dependence of a) CH* chemiluminescence amplitude and b) velocity-CH* chemiluminescence phase angle on amplitude of velocity oscillations at several equivalence ratios. Uncertainty in phase angle for $u'/u_0 < 0.05$, $\Delta\theta \sim 30$ deg; for $u'/u_0 > 0.05$, $\Delta\theta \sim 2$ deg ($f_{drive} = 300$ Hz).

40 deg from $0.05 < u'/u_0 < 0.15$. At larger disturbance amplitude, the phase decreases somewhat and then levels off. Note that the phase exhibits amplitude dependence at disturbance levels significantly lower than the gain. It is likely that the monotonic phase increase in the $0.05 < u'/u_0 < 0.15$ region is caused by the lengthening of the flame with increased disturbance amplitudes. Because of the strong similarity in both the CH* and OH* results, only CH* results are presented in the remainder of the paper.

A. Equivalence Ratio Dependence

Figure 8a presents the dependence of CH*' upon u' for equivalence ratios ranging from 0.83 to 0.90. The maximum driving amplitude point is not caused by actuator limitations, but flame blowoff. It is clearly seen that the slope in the linear regime as well as the CH* saturation amplitude decreases as the equivalence ratio is decreased. The results also show that the blowoff velocity oscillation amplitude for the majority of tests is approximately constant except for the leanest case investigated, $\phi = 0.83$. This result clearly shows that the saturation amplitude is a function of the equivalence ratio. For equivalence ratios between 0.87 and 0.9, the velocity-CH* relationship is highly nonlinear, whereas the richest ($\phi = 0.95$, not shown) and leanest cases investigated show little nonlinearity, presumably because blowoff occurs before saturation. Figure 8b presents the corresponding phase relationship between u' and CH*'. In most cases, the phase angle initially increases to a maximum and then decreases or stays roughly constant with increase in velocity oscillation amplitude.

B. Driving Frequency Effects

In addition to varying the equivalence ratio, the effect of driving frequency between 260 and 320 Hz was extensively analyzed. This range was chosen because of the high-quality data that could be obtained at these frequencies as a result of the large flame response [see Fig. 5] and its proximity to a 310-Hz combustor resonance (discussed further next). Figure 9 presents the dependence of the CH*

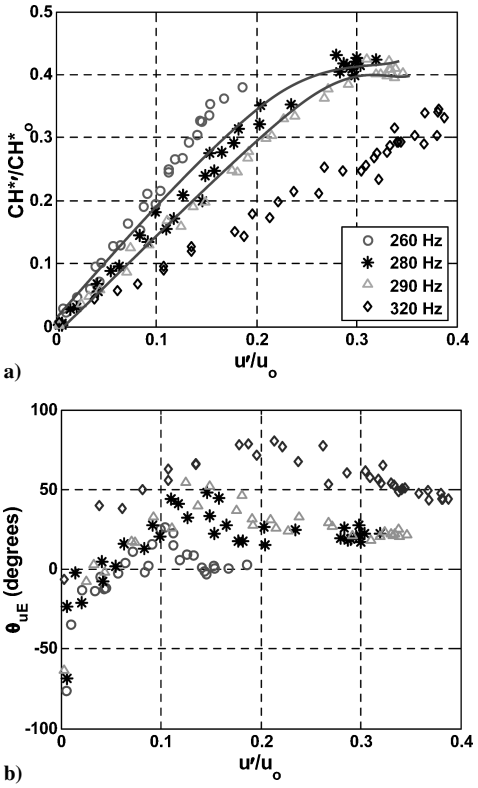

Fig. 9 Dependence of CH* chemiluminescence a) amplitude and b) phase upon velocity amplitude at several driving frequencies. Uncertainty in phase angle for $u'/u_0 < 0.05$, $\Delta\theta \sim 30$ deg; for $u'/u_0 > 0.05$, $\Delta\theta \sim 2$ deg ($\phi = 0.95$).

amplitude and phase upon u'/u_0 over the 260- to 320-Hz frequency range. Note that the slopes of these curves in the linear region are equal to the transfer function values plotted in Fig. 5. Nonlinearities in the CH*-u' gain relationship are prominent in the 280- and 290-Hz driving cases, whereas the transfer function is substantially more linear at the other frequencies. The near linearity of the transfer function in other cases all of the way to flame blowoff strongly suggests that nonlinearity is not caused by flame holding; if flame holding were a key nonlinear mechanism, one would expect the transfer function at all frequencies and equivalence ratios to become nonlinear near the blowoff point. The normalized CH* fluctuations at the point where nonlinearity is evident have similar values for 280 and 290 Hz, but the corresponding velocity amplitudes appear to vary slightly with driving frequency. Figure 9b shows that the phase exhibits similar amplitude dependence as in the equivalence ratio results. Again, note that nonlinearity is evident in the phase behavior at very low amplitudes, for example, $u'/u_0 \sim 0.05$, where the gain is still very linear.

C. Harmonic and Subharmonic Characteristics

In addition to characterizing the dependence of the flame transfer function on the fundamental driving frequency, extensive analysis of the higher and subharmonics of the dynamic signals was performed. Prior studies suggest that such data are needed to obtain a comprehensive understanding of the nonlinear combustion process. For example, it is well established from forced response studies in various mixing layers, jets, and wakes that such understanding is key to the system's nonlinear dynamics (e.g., see Ref. 34). These amplitudes are substantially smaller than those of the fundamental, however, resulting in reduced coherence between the fundamental and first harmonic, $\gamma_{i=f,j=2f}$. As such, only a single subharmonic and harmonic of the chemiluminescence signal ($CH^{*\prime}_{f=\text{fdrive}/2}$ and $CH^{*\prime}_{f=2\text{fdrive}}$) could be accurately quantified. The first subharmonic as well as the first and second harmonics of the pressure signal could be quantified because of much higher coherence values. Although the presence of higher harmonics in the data could be either to actuator or combustion process nonlinearities, analysis of our data

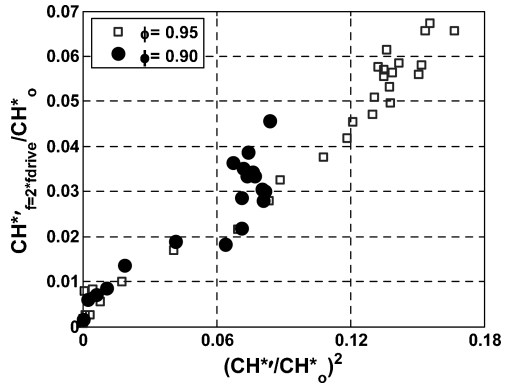

Fig. 10 Dependence of CH* first harmonic on the square of CH* fundamental at two equivalence ratios ($f_{\text{drive}} = 300$ Hz).

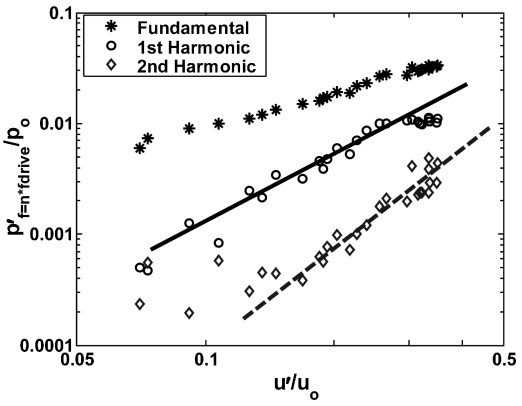

Fig. 11 Dependence of pressure harmonic amplitude on velocity oscillation amplitude ($f_{\text{drive}} = 290$ Hz, $\phi = 0.95$): ——, quadratic trend, - - - -, cubic trend.

indicates that the dominant source of harmonic generation can be attributed to the nonlinear combustion process.

First harmonic characteristics of the CH* oscillations are presented in Fig. 10 for two equivalence ratios, $\phi = 0.95$ and $\phi = 0.90$ at a driving frequency of 300 Hz. These two cases present examples where the flame transfer function remained linear throughout the range of disturbance amplitudes as well as where the flame transfer function saturated at large amplitudes of velocity oscillations. Figure 10 illustrates that the first harmonic behavior can change markedly between linear and nonlinear cases. For the linear case, $\phi = 0.95$, the first harmonic of the chemiluminescence exhibits a quadratic behavior on the fundamental throughout. This result is indicative of the other cases where the transfer function remains linear. For nonlinear cases, however, the functional relationship between the first harmonic and the fundamental changes. At low disturbance amplitudes, the general quadratic behavior is followed for $\phi = 0.90$. At forcing amplitudes above the saturation point of the fundamental, however, the first harmonic has been found to exhibit a variety of behaviors. For $\phi = 0.90$, the first harmonic deviates from the quadratic dependence, by increasing much more rapidly. In other cases, the first harmonic increases more slowly than the quadratic dependence, such as can be seen in the pressure in Fig. 11. The quadratic dependence between the fundamental and first harmonic is more clearly evident in the pressure data, which has a much higher signal-to-noise ratio. We have also found that the amplitude of the second harmonic of the pressure (because of its higher coherence values) is essentially proportional to the third power of the fundamental, as might be expected (see Fig. 11). Figure 12 presents the phase angle between the CH* chemiluminescence fundamental and first harmonic. Although the overall phase dependence upon disturbance amplitude is approximately linear at each driving frequency, the amplitude dependence of the phase-angle slope switches signs between 290 and 300 Hz. Furthermore, there is substantial amplitude dependence of this phase angle, as it changes by over 800 deg.

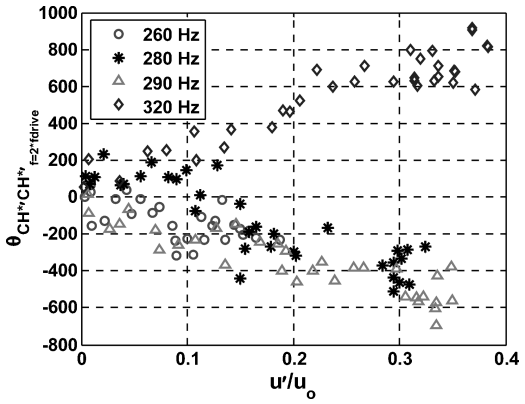

Fig. 12 Dependence of CH* chemiluminescence fundamental first harmonic phase angle on velocity oscillation amplitude at several driving frequencies ($\phi = 0.95$). Uncertainty in phase angle for $u'/u_0 < 0.05$, $\Delta\theta \sim 30$ deg; for $u'/u_0 > 0.05$, $\Delta\theta \sim 3$ deg.

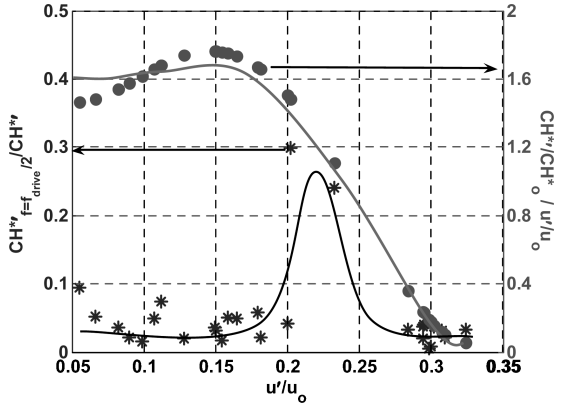

Fig. 13 Dependence of CH* subharmonic and transfer function gain on velocity oscillation amplitude ($f_{drive} = 280$ Hz, $\phi = 0.95$).

Consider next the CH* subharmonic characteristics, that is, $CH^*_{f=\text{fdrive}/2}$. In contrast to the higher harmonic characteristics, the subharmonic amplitudes do not exhibit a power-law dependence upon the fundamental at low or high disturbance amplitudes. Its amplitude jumps up, however, in the vicinity of the point where the fundamental saturates, as shown in Fig. 13. Figure 13 illustrates the dependence of the CH* chemiluminescence subharmonic on the amplitude of velocity oscillations for one case where the flame transfer function saturates, 280 Hz. In addition to the subharmonic, this figure also illustrates the gain of the flame transfer function over the entire range of disturbance amplitudes.

For this case, the subharmonic amplitudes are very low and incoherent with respect to the fundamental when the corresponding transfer function is in the linear regime ($u'/u_0 < 0.2$). Coherence values around 0.6–0.7 for these low values will create uncertainties that are as large as or larger than the values themselves. As the transfer function approaches the saturation point (approximately $u'/u_0 \sim 0.2$ for the case illustrated), the subharmonic exhibits a sharp increase in amplitude. At this point, the coherence between the subharmonic and fundamental has values of ~0.99. Corresponding plots of the velocity and pressure subharmonics show no such increase and remain incoherent. After this sharp increase, the subharmonic amplitude decreases sharply and is again quite incoherent with the fundamental. This discontinuous dependence of the subharmonic on the fundamental is exhibited for all cases where saturation of the transfer function occurs. However, the presence of subharmonic oscillations does not always accompany saturation. There were some cases where a peak in the CH* subharmonic occurred when the flame transfer function remained linear. This peak in the chemiluminescence subharmonic was accompanied by similar peaks in the velocity and pressure subharmonics, in contrast to the cases just described.

The subharmonic's dependence upon amplitude is very similar to the measurements of Bourehla and Baillot[26] in a laminar, Bunsen flame. At intermediate forcing amplitudes, they observed, in some cases, a subharmonic flame response. Analysis of this response showed that the subharmonic amplitude increased and the fundamental amplitude decreased as one went downstream from the burner lip. That is, the flame base responded more at the fundamental frequency, and the flame tip responded more to the subharmonic. In all cases, the subharmonic response disappeared at the highest forcing amplitudes, and the flame because hemispherical. This phenomenon appears to be manifestation of the so-called parametric instability, where pulsating cellular structures appear on the flame, which oscillate at half the instability frequency.[35–38] Analogous to Bourehla and Baillot's result, these studies in nominally flat flames found the subharmonic response only at intermediate amplitudes; at very high amplitudes the flame response was highly chaotic and disordered.

This instability is produced by the unsteady acceleration of the flame front by the velocity field, which separates two regions of differing densities, coupling with the three-dimensional flame dynamics. With increased amplitudes, the structures lose their well-defined nature and break up into disordered, turbulent wrinkles. This period doubling was recognized by Markstein[34] as indicative of a parametrically pumped oscillator that can be described by an equation of the form:

$$A\frac{\mathrm{d}^2 y(k,y)}{\mathrm{d}t^2} + B\frac{\mathrm{d}y(k,y)}{\mathrm{d}t} + [C_0 - C_1\cos(\omega t)]y(k,t) = 0 \quad (2)$$

where A, B, C are coefficients defined by Markstein, k is the wave number of the perturbation, and ω is the frequency of the imposed oscillations. The damping coefficient B is always positive, but the coefficient C_0 is negative if the nominal planar flame front is unstable. Such an equation has the well-known property that subharmonic oscillations (i.e., $\omega/2$) are excited for large enough parametric disturbance amplitudes C_1.

This is the first observation, to the authors' knowledge, of the presence of the parametric instability in a swirl-stabilized turbulent flame. Vaezi and Aldredge[38] have performed experimental work analyzing the parametric instability during turbulent flame propagation. They found substantial enhancement of axial and circumferential velocity fluctuations as a result of the parametric instability for all levels of pre-ignition turbulence. Also, the magnitude of amplification decreased with increasing Reynolds number. In our experiments, the Reynolds number defined by the premixer exit diameter was substantially larger than those investigated by Vaezi and Aldredge.[38] Analogous to their results, no sudden visible changes in the flame position, length, or shape were noted before saturation of the transfer function occurred, which indicated that turbulent flame speed enhancement was minimal. However, it appears highly probable that nonlinear interactions between the flow forcing and parametric instability (possibly through its impact on the fluctuating flame position) are responsible for saturation of the flame response. This is evidenced by the fact that 1) the jump in subharmonic amplitude occurs at essentially the same value as that at which saturation occurs, and 2) subharmonic oscillations are always present in cases where saturation of the fundamental occur.

D. Nonlinear Heat Release—Linear Acoustics Interaction

It has been argued that the dynamics of an unstable combustor are dominated by heat-release nonlinearities, which interact with linear acoustic processes. Because the combustor is a reverberant acoustic environment, it possesses a number of acoustic modes. Many researchers (e.g., see Culick,[15] Zinn and Powell,[13] and Culick and Yang[40]) have shown that the dynamics of each mode can be described by an oscillator equation of the form:

$$\ddot{\eta}_i + 2\zeta\omega_0\dot{\eta}_i + \omega_0^2\eta_i = F(\eta_i, \dot{\eta}_i) + E(t) \quad (3)$$

where ω_0 is the linear natural frequency, ζ is the damping coefficient, $F(\eta_i, \dot{\eta}_i)$ refers to the system nonlinearities, and $E(t)$ is the external excitation.

Before presenting further data, we briefly summarize several classical results for a nonlinear system that is externally forced at a

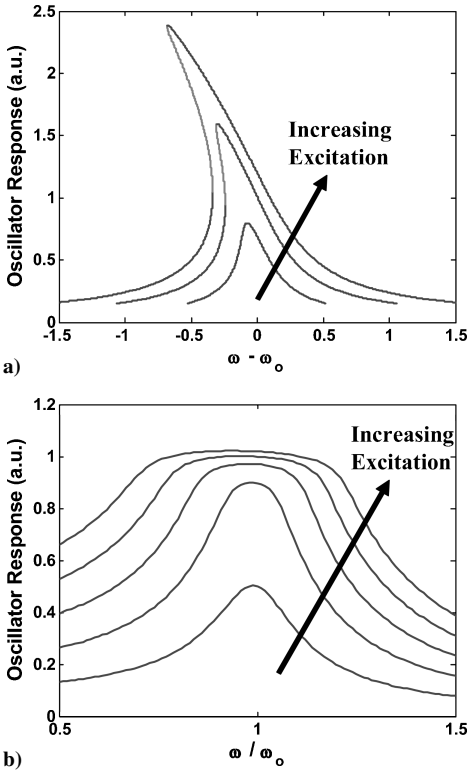

Fig. 14 Frequency–response curves at several excitation amplitudes for a second-order oscillator with nonlinearities in a) stiffness and b) damping.

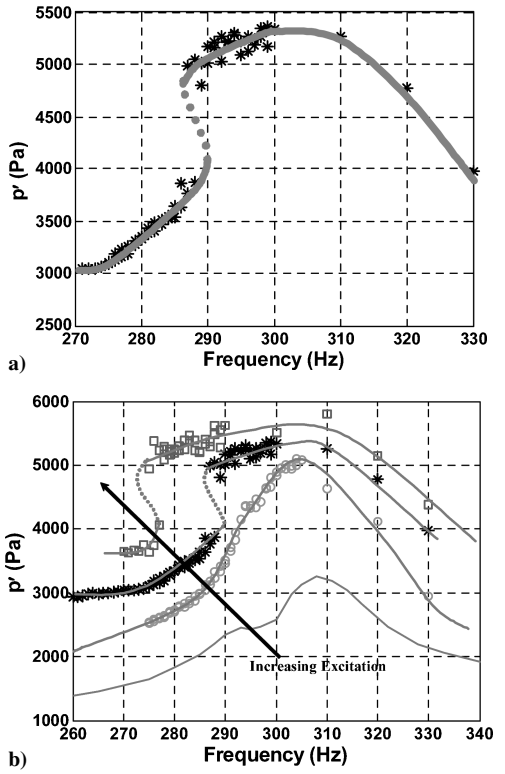

Fig. 15 Dependence of pressure amplitude upon frequency at a) a single disturbance amplitude, 2.8 A, and b) several disturbance amplitudes, 1.8–3.0 A ($\phi = 0.95$).

frequency near resonance, that is, $E(t) = A\cos\omega t$, where $\omega \approx \omega_0$. Consider first nonlinearities in "stiffness," that is, $F = F(\eta_i)$. It is well known that such a system exhibits "bending" in the frequency response curve, such as shown in Fig. 14a. As such, the frequency of the maximum oscillator response shifts with frequency, for example, increases/decreases in the effective stiffness with increasing disturbance amplitude cause the curve to bend toward higher/lower frequencies. As the frequency of the large-amplitude excitation is swept, the response of the nonlinear system follows one branch of the curves to a bifurcation point where the system jumps discontinuously to the other branch. This manifests itself in hysteresis in frequency and amplitude where this jump occurs.

Consider next nonlinearities in damping, that is, $F = F(\dot{\eta}_i)$. The peak amplitude of this type of nonlinear system will not increase proportionally to the disturbance amplitude. If damping grows nonlinearly, amplitude saturation causes a flattening of the response curve around the resonant frequency. Therefore, the maximum response is distributed over a broader range of frequencies than a linear damped oscillator, for example, see the example in Fig. 14b. Further details are in Nayfeh and Mook.[41]

Both types of behavior illustrated in Fig. 14 were observed in our data. A representative result is shown in Fig. 15a, which plots the frequency dependence of the pressure amplitude at a large disturbance amplitude. The pressure amplitude response bends over to the left indicative of a softening spring. Second, the pressure amplitude jumps in the 285–290-Hz range, with hysteresis in the frequency value where this jump occurs. Third, the peak response of the pressure remains relatively constant over a range of driving frequencies, indicating nonlinearity in damping. This behavior can be seen more clearly in Fig. 15b, which plots similar results at several driving amplitudes. The plot clearly shows the progressive trend away from a classical forced-resonant linear system at low disturbance amplitudes to a response that bends over toward lower frequencies and flattens in response.

If the forcing frequency is held constant, while the excitation amplitude is varied, a similar bifurcation occurs as shown in Fig. 16. Figure 17 shows that the pressure oscillation data have a similar dependence on frequency. As just noted, the linear natural frequency

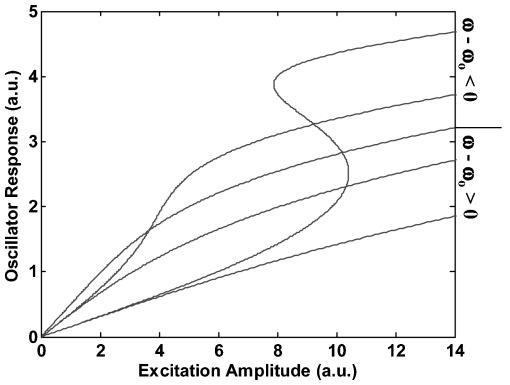

Fig. 16 Excitation–response curves for softening spring oscillator at several excitation frequencies.

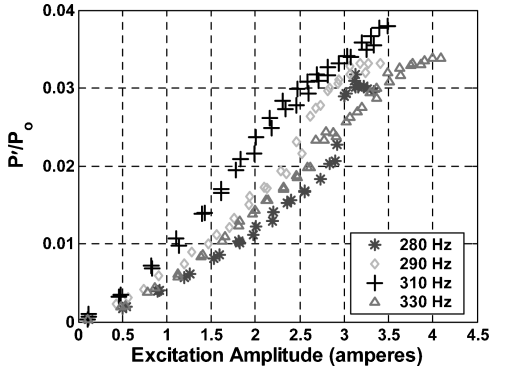

Fig. 17 Dependence of pressure oscillation amplitude on excitation amplitude for varying driving frequencies ($\phi = 0.95$).

is approximately 310 Hz. At 280 Hz there is a noticeable jump in the pressure response. At frequencies below and above 310 Hz, the pressure response exhibits a quadratic and square-root dependence upon excitation amplitude.

Referring back to Fig. 9a, note the clear saturation of the CH*-velocity transfer function at 280 Hz. Referring to the specific data points, note that a clear "gap" in the velocity amplitude is observed at a point coinciding with that where saturation is observed. The driving levels were increased in a regular, stepwise fashion over the whole range of amplitudes. This jump in the velocity coincides with the jump in pressure amplitude illustrated in Fig. 15a that is, the jump in pressure and velocity coincides with the point where the heat-release response exhibits nonlinearity.

A detailed study of this bifurcation and the associated hysteresis was performed in the 280–290-Hz frequency range. Figure 18 summarizes the amplitude-frequency parameter regions where single and multivalued behaviors occur. Hysteresis occurs at driving amplitudes larger than about 2.6 A and extends all of the way to 3.1A, where blowout occurred. The corresponding frequencies range from 292 to 276 Hz at the low- and high-amplitude driving ranges.

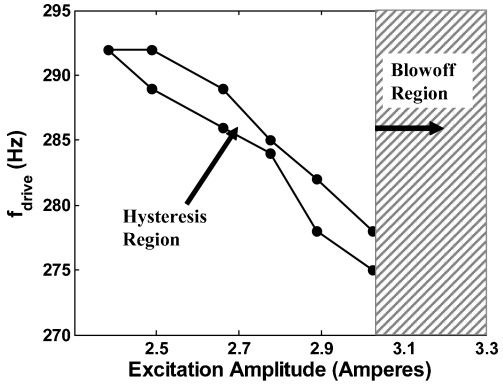

Fig. 18 Amplitude-frequency ranges over which the chemiluminescence-pressure-velocity relationship exhibited single and multivalued behavior.

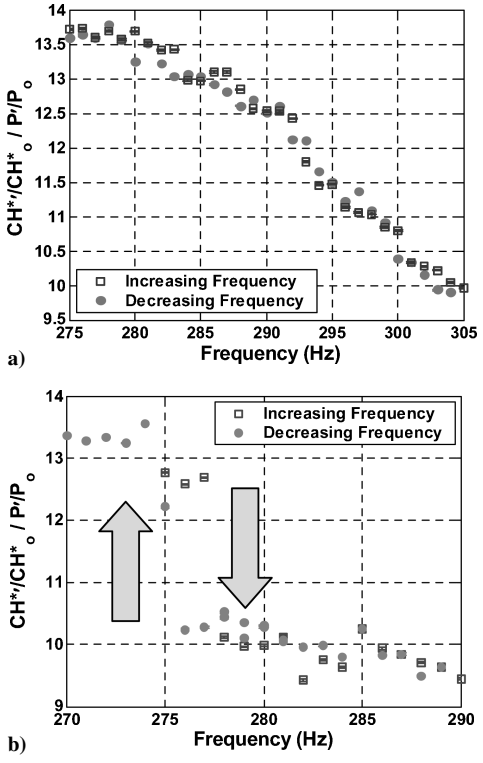

Fig. 19 Dependence of pressure-CH* transfer function on driving frequency [a) excitation amplitude = 2.4 A and b) excitation amplitude = 3.0 A, $\phi = 0.95$].

Figure 19 provides a further visualization of this bifurcation by quantifying the CH*-pressure transfer function as a function of frequency at fixed driving amplitudes. (We illustrate the CH*-pressure relationship here due to the fact that the uncertainty values are smaller than those for the velocity measurements; the trends, however, are identical.) The figure plots these dependencies at both a low and high driving amplitude of 2.4 and 3.0 A. For low driving amplitudes, the transfer function exhibits a smooth, monotonically decreasing dependence upon frequency, as would be anticipated by the results shown in Fig. 5. However, when the driving amplitude is increased beyond the cutoff point of 2.6 A, the transfer function changes markedly. This result is illustrated in Fig. 19b, where a clear jump in the transfer function values occurs (∼14% for the CH*-pressure transfer function value) for the 3.0-A driving case. Note that the frequency dependence of the transfer function is much "flatter" in the high driving case. The frequency where the jump occurs depends upon the direction of frequency change (increasing/decreasing) with a total hysteresis of about 3 Hz. Note that the transfer function itself does not exhibit a discontinuous dependence upon amplitude; rather, the pressure amplitude exhibits a discontinuity in the region where the transfer function changes. This transfer function change is responsible for the bifurcation in pressure amplitude. As such, it is not possible to measure a monotonic change in the transfer function at these frequencies because of the discontinuous jumps that occur in acoustic amplitude. A similar result is found in the corresponding phase relationships.

V. Conclusions

From these data, several conclusions can be drawn regarding the nonlinear response of the unsteady heat release to flow perturbations. The amplitude relationship between the pressure/velocity and heat release saturates at sufficiently high forcing levels at certain frequencies and equivalence ratios, but remains linear at others all of the way to flame blowout. Also, substantial amplitude dependence of the CH* phase was found at all driving frequencies and equivalence ratios, clarifying the questions raised by Lieuwen and Neumeier.[24] These results suggest that heat-release-acoustic nonlinearities in both gain and phase can play comparable roles in swirling, premixed combustors. Although the measured flame transfer functions themselves are independent of the system's acoustics, a bifurcation in pressure amplitude occurs around the natural frequency that is introduced by the nonlinear combustion process.

One of the key conclusions of this study is that nonlinear interactions between the flow forcing and parametric instability (possibly through its impact on the fluctuating flame position) might be responsible for saturation of the flame response. The presence of the parametric instability is manifested by the jump in amplitude of oscillations at half the driving frequency at certain disturbance amplitude values. This jump in subharmonic amplitude occurs at essentially the same value as that at which saturation occurs. Furthermore, subharmonic oscillations are always present in cases where saturation of the fundamental occurs. To our knowledge, this observation of the parametric instability is the first in a turbulent, swirl-stabilized flame.

In addition, however, there are other potential mechanisms that might also be present. These include local extinction of the flame and flame sheet kinematics. For example, increaing amplitudes of oscillation lead to increased flame strain, which could cause local flame extinction events. Increased extinction could, in turn, result in decreased heat-release response. This mechanism could be responsible for the decreasing mean chemiluminescence levels upon perturbation amplitude seen in some test cases. Additionally, flame sheet kinematics also might be important. Although their significance was alluded to earlier in the context of the parametric flame instability (i.e., fluctuating flame position effects), they can play additional roles through nonlinear dependencies of flame area destruction with disturbance amplitude. For example, large-amplitude corrugations of the flame can be consumed by flame propagation faster than small-amplitude perturbations, emphasized by Preetham and Lieuwen[5] based on theoretical considerations and very recently, by Balachandran et al.,[27] based on experimental imaging studies.

Although it is not possible to conclusively determine the relative roles of all potential mechanisms of nonlinearity, we can eliminate some mechanisms that have been suggested as potentially significant:

1) **Global extinction**—This is the mechanism proposed by Dowling[17] and Poinsot et al.,[20] which follows from the simple observation that the instantaneous heat release cannot go negative, thus limiting the chemiluminescence fluctuations to 100% of the mean value. Our data indicate saturation at substantially lower amplitudes, however, implying that this mechanism is not significant in this combustor.

2) **Chemical kinetics**—Reaction rates depend upon pressure and temperature in a nonlinear manner. These nonlinearities will apparently become significant when the fluctuating pressure and temperature achieve amplitudes on the order of their mean values. This mechanism does not appear likely here, however, as nonlinearity occurs at p'/p_0 values of $\sim 2\%$.

3) **Equivalence ratio oscillations**—The nonlinear dependence of the equivalence ratio amplitude and heat-release response discussed by Peracchio and Proscia[18] and Lieuwen[16] is not important here, as the fuel/air mixture had a constant composition. As such, though we cannot comment on the magnitude of these types of nonlinearities in situations where they are present, the data presented here indicate that other flame processes also cause nonlinearities in flame response.

4) **Flame holding**—The many data indicating a linear CH^* response all of the way to blowoff indicate that nonlinearities caused by marginal flame holding are probably not important.

References

[1]Cohen, J., and Anderson, T., "Experimental Investigation of Instabilities in a Lean, Premixed Step Combustor," AIAA Paper 96-0819, 1996.

[2]Straub, D. L., and Richards, G. A., "Effect of Fuel Nozzle Configuration on Premix Combustion Dynamics," American Society of Mechanical Engineers, Paper 98-GT-492, June 1998.

[3]Paschereit, C. O., Gutmark, E., and Weisenstein, W., "Control of Thermo-Acoustic Instabilities and Emissions in an Industrial Type Gas Turbine Combustor," *Proceedings of the Combustion Inst*., Aug. 1998, pp. 1817–1824.

[4]Hsiao, G. C., Pandalai, R. P., Hura, H. S., and Mongia, H. C., "Combustion Dynamic Modeling for Gas Turbine Engines," AIAA Paper 98-3380, 1998.

[5]Preetham, Lieuwen, T., "Nonlinear Flame-Flow Transfer Function Calculations: Flow Disturbance Celerity Effects Part 2," AIAA Paper 2005-0543, Jan. 2005.

[6]Crocco, L., and Cheng, S., *Theory of Combustion Instability in Liquid Propellant Rocket Motors*, Butterworths, London, 1956.

[7]Munjal, M., *Acoustics of Ducts and Mufflers*, Wiley, New York, 1987.

[8]Fleifil, M., Annaswamy, A. M., Ghoniem, Z. A., and Ghoniem, A. F., "Response of a Laminar Premixed Flame to Flow Oscillations: A Kinematic Model and Thermoacoustic Instability Results," *Combustion and Flame*, Vol. 106, 1996, pp. 487–510.

[9]Ducruix, S., Durox, D., and Candel, S., "Theoretical and Experimental Determinations of the Transfer Function of a Laminar Premixed Flame," *Proceedings of the Combustion Inst*., Vol. 28, 2000.

[10]Kruger, U., Hüren, J., Hoffman, S., Krebs, W., and Bohn, D., "Prediction of Thermoacoustic Instabilities with Focus on the Dynamic Flame Behavior for the 3A-Series Gas Turbine of Siemens KWU," American Society of Mechanical Engineers, Paper 99-GT-111, June 1999.

[11]Walz, G., Krebs, W., Hoffman, S., and Judith, H., "Detailed Analysis of the Acoustic Mode Shapes of an Annular Combustion Chamber," American Society of Mechanical Engineers, Paper 99-GT-113, June 1999.

[12]Schuermans, B. H., Polifke W., and Paschereit, C. O., "Modeling Transfer Matrices of Premixed Flames and Comparison with Experimental Results," American Society of Mechanical Engineers, Paper 99-GT-132, June 1999.

[13]Zinn, B. T., and Powell, E. A., "Nonlinear Combustion Instability in Liquid-Propellant Rocket Engines," *Proceedings of the Combustion Inst*., Vol. 13, Aug. 1970, pp. 491–503.

[14]Culick, F. E. C., Burnley, V., and Swenson, G., "Pulsed Instabilities in Solid-Propellant Rockets," *Journal of Propulsion and Power*, Vol. 11, No. 4, 1995, pp. 657–665.

[15]Culick, F. E. C., "Non-Linear Growth and Limiting Amplitude of Acoustic Oscillations in Combustion Chambers," *Combustion Science and Technology*, Vol. 3, No. 1, 1971, pp. 1–17.

[16]Lieuwen, T., "Experimental Investigation of Limit Cycle Oscillations in an Unstable Gas Turbine Combustor," *Journal of Propulsion and Power*, Vol. 18, No. 1, 2002, pp. 61–67.

[17]Dowling, A. P., "Nonlinear Self-Excited Oscillations of a Ducted Flame," *Journal of Fluid Mechanics*, Vol. 346, 1997, pp. 271–290.

[18]Peracchio, A. A., and Proscia, W. M., "Nonlinear Heat Release/Acoustic Model for Thermo-Acoustic Instability in Lean Premixed Combustors," *Journal of Engineering for Gas Turbines and Power*, Vol. 121, 1999.

[19]Wu, X., Wang, M., Moin, P., and Peters, N., "Combustion Instability due to the Nonlinear Interaction Between Sound and Flame," *Journal of Fluid Mechanics*, Vol. 497, 2003, pp. 23–53.

[20]Poinsot, T., Veynante, D., Bourienne, F., Candel, S., Esposito, E., and Surget, J., "Initiation and Suppression of Combustion Instabilities by Active Control," *Proceedings of the Combustion Inst*., Vol. 22, Aug. 1988, pp. 1363–1370.

[21]Dowling, A. P., "A Kinematic Model of a Ducted Flame," *Journal of Fluid Mechanics*, Vol. 394, Aug. 1999, pp. 51–72.

[22]Searby, G., "Acoustic Instability in Premixed Flames," *Combustion Science and Technology*, Vol. 81, No. 4-6, 1992, pp. 221–231.

[23]Külsheimer, C., and Büchner, H., "Combustion Dynamics of Turbulent, Swirling Flows," *Combustion and Flame*, Vol. 131, No. 1-2, 2002, pp. 70–84.

[24]Lieuwen, T., and Neumeier, Y., "Nonlinear Pressure-Heat Release Transfer Function Measurements in a Premixed Combustor," *Proceedings of the Combustion Inst*., Vol. 29, July 2002, pp. 99–105.

[25]Lee, J. G., and Santavicca, D., "Experimental Diagnostics for the Study of Combustion Instabilities in Lean, Premixed Gas Turbine Combustors," *Journal of Propulsion and Power*, Vol. 19, No. 5, 2003, pp. 737–750.

[26]Bourehla, A., and Baillot, F., "Appearance and Stability of a Laminar Conical Premixed Flame Subjected to an Acoustic Perturbation," *Combustion and Flame*, Vol. 114, No. 3-4, 1998, pp. 303–318.

[27]Balachandran, R., Ayoola, B. O., Kaminski, C. F., Dowling, A. P., and Mastorakos, E., "Experimental Investigation of the Nonlinear Response of Turbulent Premixed Flames to Imposed Velocity Oscillations," *Combustion and Flame*, Vol. 143, No. 1-2, 2005, pp. 37–55.

[28]Durox, D., Baillot, F., Searby, G., and Boyer, L.,"On the Shape of Flames Under Strong Acoustic Forcing: A Mean Flow Controlled by an Oscillating Flow," *Journal of Fluid Mechanics*, Vol. 350, 1997, pp. 295–310.

[29]Lieuwen, T., Torres, H., Johnson, C., Daniel, B. R., and Zinn, B. T., "A Mechanism for Combustion Instabilities in Premixed Gas Turbine Combustors," *Journal of Engineering for Gas Turbines and Power*, Vol. 123, No. 1, 2001, pp. 182–190.

[30]Neumeier, Y., Nabi, A., and Zinn, B. T., "Investigation of the Open Loop Performance of an Active Control System Utilizing a Fuel Injector Actuator," AIAA Paper 96-2757, Jan. 1996.

[31]Broda, J. C., Seo, S., Santoro, R. J., Shirhattikar, G., and Yang, V., "An Experimental Investigation of Combustion Dynamics of a Lean, Premixed Swirl Injector," *Proceedings of the Combustion Inst*., Vol. 27, Aug. 1998, pp. 1849–1856.

[32]Bendat, J., and Piersol, A., *Random Data: Analysis and Measurement Procedures*, Wiley, New York, 1986.

[33]Schuller, T., Durox, D., and Candel, S., "A Unified Model for the Prediction of Laminar Flame Transfer Functions: Comparisons Between Conical and V-Flame Dynamics," *Combustion and Flame*, Vol. 134, No. 1-2, 2003, pp. 21–34.

[34]Coats, C., "Coherent Structures in Combustion," *Progress in Energy and Combustion Sciences*, Vol. 22, No. 5, 1996, pp. 427–509.

[35]Clavin, P., Pelce, P., and He, L., "One-Dimensional Vibratory Instability of Planar Flames Propagating in Tubes," *Journal of Fluid Mechanics*, Vol. 216, 1990, pp. 299–322.

[36]Searby, G., and Rochwerger, D., "A Parametric Acoustic Instability in Premixed Flames," *Journal of Fluid Mechanics*, Vol. 231, 1991, pp. 529–543.

[37]Vaezi, V., and Aldredge, R. C., "Laminar Flame Instabilities in a Taylor-Couette Combustor," *Combustion and Flame*, Vol. 121, No. 1-2, 2000, pp. 356–366.

[38]Vaezi, V., and Aldredge, R. C., "Influences of Acoustic Instabilities on Turbulent-Flame Propagation," *Experimental Thermal and Fluid Science*, Vol. 20, 2000, pp. 162–169.

[39]Markstein, G., "Flames as Amplifiers of Fluid Mechanical Disturbances," *Proceedings of the Sixth National Congress on Applied Mechanics*, 1970, pp. 11–33.

[40]Culick, F. E. C., and Yang, V., "Overview of Combustion Instabilities in Liquid-Propellant Rocket Engines," *Liquid Rocket Engine Combustion Instability*, edited by V. Yang, and W. E. Anderson, Progress in Astronautics and Aeronautics, Vol. 169, 1995, Chap. 1, pp. 3–37.

[41]Nayfeh, A. H., and Mook, D. T., *Nonlinear Oscillations*, Wiley, New York, 1995.